https://doi.org/10.17221/121/2025-RAE

Research on the optimal design and process parameters of a castor seed cleaning machine

Elchyn Aliiev[1], Valentyn Holovchenko[1], Olha Aliieva[2]*

[1]Faculty of Engineering and Technology, Dnipro State Agrarian and Economic University, Dnipro, Ukraine
[2]Department of Technical and Technological Support of Seed Production, Institute of Oilseed Crops of the National Academy of Agrarian Sciences of Ukraine, Zaporizhzhia, Ukraine

**Corresponding author: aliev@meta.ua*

Citation: Aliiev E., Holovchenko V., Aliieva O. (2026): Research on the optimal design and process parameters of a castor seed cleaning machine. Res. Agr. Eng., 72: 41–58.

Abstract: In the context of the modern EU bioeconomy, the use of industrial crops, particularly castor beans (*Ricinus communis* L.), is relevant for the production of industrial and energy products without competing with food crops. Castor oil is used for the production of biodiesel, lubricants, paints and coatings, cosmetics, and pharmaceuticals. In Ukraine, castor beans can be cultivated on low-yield soils, with seed yields ranging from 1.5 t/ha to 2.1 t/ha depending on the variety. However, the morphological features of the fruits and uneven ripening complicate the mechanisation of harvesting and seed cleaning processes. Existing equipment designed for other crops cannot be applied due to the risk of damaging the castor seeds. A design of a castor seed cleaning machine has been proposed, combining mechanical fruit shelling with the aerodynamic separation of the mixture. The machine is equipped with an eccentric crushing cone, rubber linings, a pneumatic separation channel, a cyclone, and an automated control unit. As a result of numerical modelling and experimental studies of the process of separating and cleaning castor seeds, dependencies were obtained for the productivity of the developed machine Q, power consumption P, specific energy consumption E, fraction of unshelled fruits (segments) ξ_f, content of the clean seed in the seed collector $\psi_{s\text{-}s}$ depending on the distance between the reverse and crushing cones δ, rotation frequency of the crushing cone n, diameter of the feed opening D_{in}, inclination angle of the crushing cone axis γ, and airflow velocity V. A multi-criteria optimisation method was applied to find the optimal operating modes: δ = 10.8 mm; n = 282 rpm; V = 3.6 m/s; D_{in} = 98 mm; γ = 3.6°; β = 20.3°. The following results were achieved: E = 0.0394 MJ/kg; Q = 163.4 kg/h; P = 1 861 W; ξ_f = 0.099; $\psi_{s\text{-}s}$ = 0.958. The obtained results confirm the efficiency of the proposed design for industrial implementation.

Keywords: experiment; mechanical shelling; numerical simulation; productivity; quality; regression models; separation; specific energy

According to the latest bioeconomy directives issued by the European Union, the industrial sector must increasingly rely on bio-based materials instead of traditional fossil resources (Janiszewska et al. 2021; Wydra et al. 2021). The agricultural sector can contribute to this goal by improving the utilisation of by-products from oilseed crops (Román-Figueroa et al. 2020). However, the cultivation of industrial crops raises concerns regarding land use and potential competition between food

https://doi.org/10.17221/121/2025-RAE

and non-food crops (Gelfand et al. 2013). Growing industrial crops on low-yield lands may provide the most balanced solution, allowing the EU to achieve future energy goals without reducing the land available for food production (Von Cossel et al. 2019). Therefore, exploring value-added chains for low-input crops is essential for enabling their sustainable large-scale implementation.

In this context, the castor bean (*Ricinus communis* L.) has emerged as a promising non-food crop (Zanetti et al. 2013; Alexopoulou et al. 2015), capable of cultivation under low-resource conditions in Ukraine, with seed yields of 1.6–1.8 t/ha (Olesya variety), 1.7–2.1 t/ha (Khortychanka variety), and 1.5–1.7 t/ha (Khortytska 3 variety) (Vedmedeva et al. 2018). Castor oil is a versatile product, used for biodiesel, cosmetics, pharmaceuticals, paints, varnishes, lubricants for two-stroke engines, and as a component in semi-rigid polyurethane foam for thermal insulation (Ogunniyi 2006; Singh 2011; Carrino et al. 2020). Moreover, the inherent toxicity of ricin and other alkaloids in castor seeds adds safety considerations, making the careful design of the cleaning process critical to minimise exposure risks (Sousa et al. 2017; Abomughaid et al. 2024). The efficient development of a domestic castor oil supply chain could significantly reduce the EU and Ukraine's dependence on imported vegetable oils for industrial and energy purposes.

Ricinus communis L. is highly diverse, with wild and semi-cultivated types differing in genetic and phenotypic traits, sometimes reaching the height of a medium-sized tree (Anjani 2012). Seeds develop inside capsules arranged in one or more racemes, which mature gradually throughout the plant's life. Consequently, seed ripening within racemes is non-uniform (Koutroubas et al. 1999; Vallejos et al. 2011; Shevchenko and Aliiev 2022), complicating the mechanised harvesting. As specialised machinery remains limited, manual harvesting is often necessary, increasing production costs, though it remains suitable for small-scale or high-reproduction seed material (Shevchenko and Aliiev 2022).

To improve the efficiency, segmented harvesting strategies are employed, involving multiple machines to perform harvesting, transport, cleaning, and dehulling operations. These can occur either in the field or at storage sites, where fruits are first collected and transported, then dehulled and cleaned using specialised equipment. Seed damage during cleaning is a key factor, as it can lead to significant losses and reduce both the seed and oil quality (Yang et al. 2021).

Existing equipment for other crops cannot be directly applied to castor due to the high risk of seed damage. At the same time, reviewing the existing harvesting and cleaning machinery, including the operational principles, configurations, performance, advantages, and limitations, highlights the necessity of developing specialised equipment adapted to castor seeds. Based on such analyses (Cao et al. 2012; Gbabo et al. 2015; Li et al. 2016; He 2018; Hou et al. 2018; Yakubu et al. 2020), five main groups (Figure 1) of working principles for castor dehulling and seed separation machines can be distinguished (Tesliuk and Holovchenko 2025).

The first group includes machines where fruits are dehulled by friction and compression between abrasive disks or between a stationary plate and a rotating roller, with movement trajectories and exposure times varying by design; examples include vertical-axis disk dehullers and roller-plate machines. The second group uses prolonged friction between the fruits and abrasive surfaces to remove the outer shells, requiring the working zone to be filled, typically with horizontal shafts. The third group relies on repeated impacts and inertial forces, achieved via rotating beaters or centrifugal devices, to break and separate shells. The fourth group employs shear and compression forces using pairs of rubber-coated rollers rotating in opposite directions at different speeds. Finally, the fifth group comprises air-assisted dehullers, where high-speed air streams create pressure differences, tangential forces, and compression jumps to remove shells without moving mechanical parts.

Despite their importance, the seed damage and cleaning efficiency have not been fully addressed in previous studies. Understanding these effects is essential for designing and optimising castor seed cleaning machinery, particularly due to the distinct rheological properties of castor seeds compared to other crops (Yang et al. 2021; Aliiev and Holovchenko 2025). Therefore, developing a castor seed cleaning machine and justifying its design and process parameters represents a relevant applied scientific task. The purpose of this research is to improve the efficiency of castor seed separation and cleaning by substantiating the technological process, parameters, and operating modes of the separator-cleaner based on the seeds' rheological characteristics.

https://doi.org/10.17221/121/2025-RAE

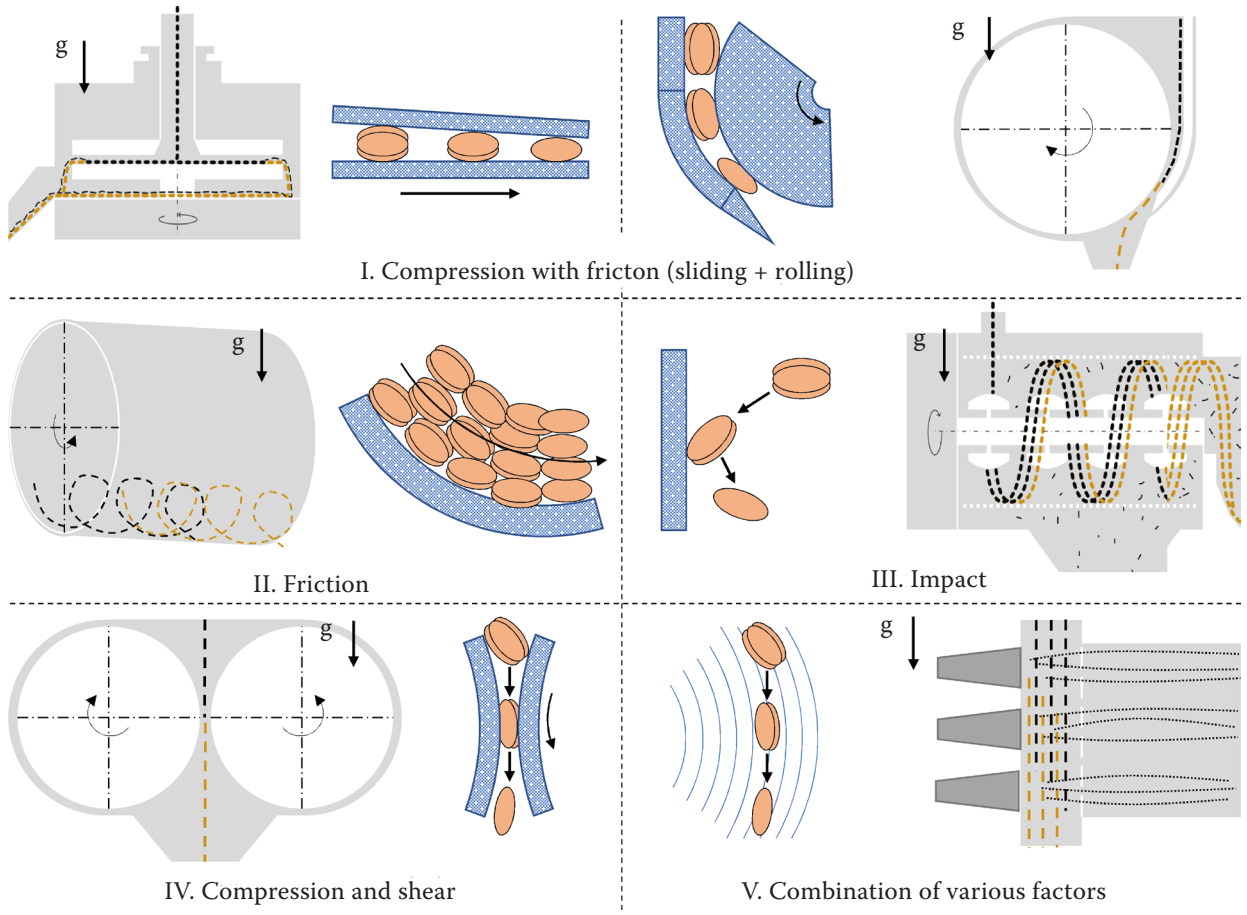

Figure 1. Classification of the main working-zone designs of machines for castor fruit dehulling and seed separation (Tesliuk et al. 2025)

MATERIAL AND METHODS

Design description. The castor seed cleaning machine (Figure 2) consists of a frame whose main component is a reverse cone, which includes a housing with an internal lining, four adjusting screws, four sprockets, and a chain. The loading hopper comprises a container and a bar-type grid. The crushing cone consists of an outer lining, a distributor, and a conical shaft.

The drive system includes a conical eccentric sleeve-shaft, an angular gearbox, driven and driving pulleys, a belt, and the main electric motor. The machine is also equipped with an aerodynamic cleaning system, which comprises a chute located under the crushing cone, a pneumatic separation channel with a sieve at the bottom, a seed collector under the sieve, a collector for unhulled fruits beyond the sieve, and a cyclone connected to the upper part of the pneumatic separation channel. There are also collectors for capsule fragments and fine particles with dust, connected to the cyclone. Additionally, the system includes a centrifugal fan and a fan electric motor.

A motor-reducer shaft is attached to the upper end of one of the four adjusting screws, with the motor-reducer mounted on the housing with the internal lining. Furthermore, the machine is equipped with a control unit, connected via electrical wires to the motor-reducer, main electric motor, and fan motor.

The developed design of the castor seed cleaning machine offers several advantages that ensure its effective operation. First and foremost, it performs comprehensive cleaning by combining mechanical fruit shelling with the subsequent aerodynamic separation of the mixture components. Thanks to the control unit, the operator can precisely adjust the main process parameters, including the rotational speed of the crushing cone, the fan capacity, and the gap between the housing's internal

https://doi.org/10.17221/121/2025-RAE

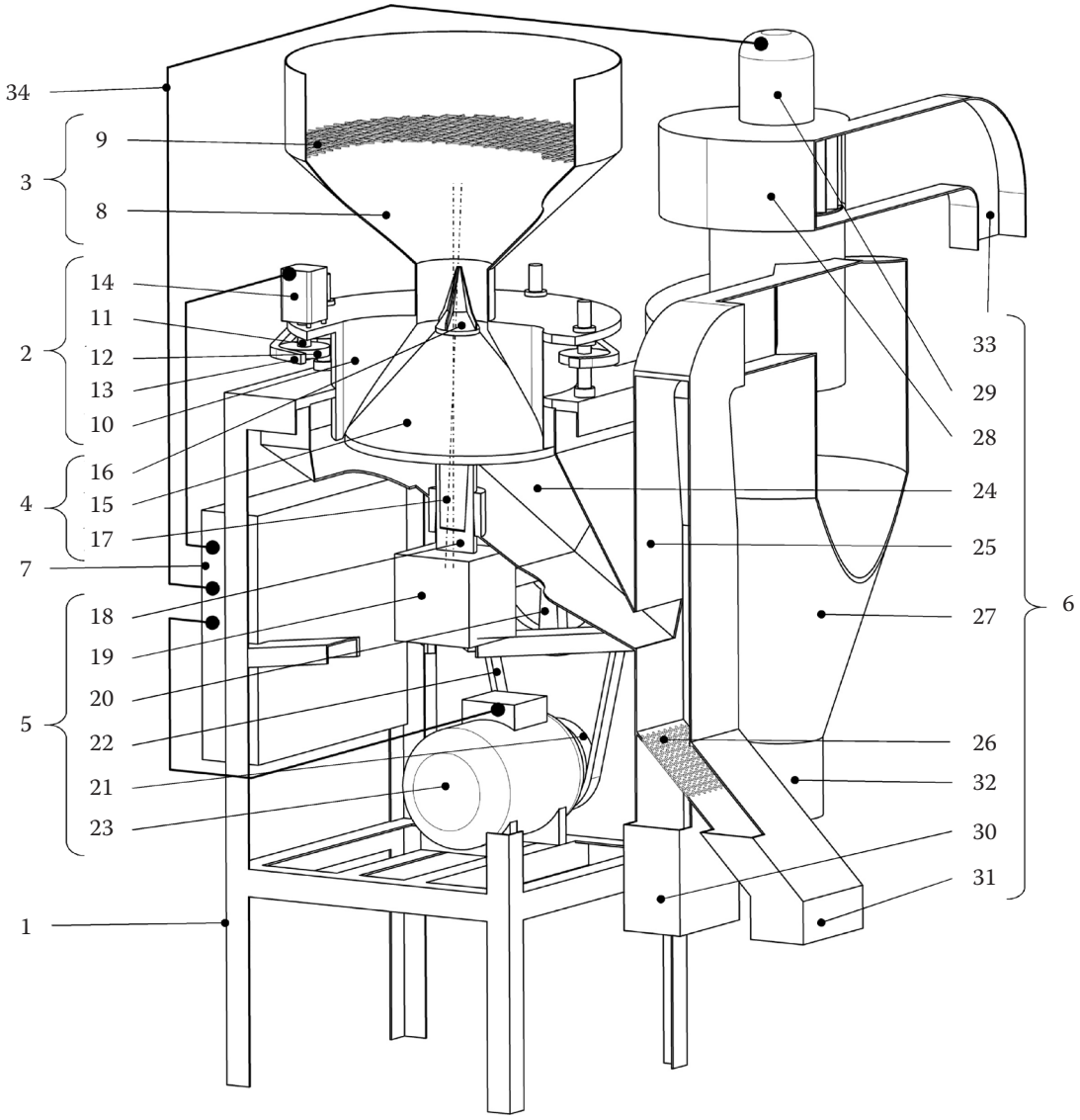

Figure 2. General view of the castor seed cleaning machine

1 – frame; 2 – reverse cone; 3 – loading hopper; 4 – crushing cone; 5 – drive; 6 – aerodynamic cleaning system; 7 – control unit; 8 – container; 9 – rod screen; 10 – housing with internal lining; 11 – adjustment screw; 12 – sprocket; 13 – chain; 14 – motor reducer; 15 – external lining; 16 – distributor; 17 – conical shaft; 18 – conical eccentric cup-shaft; 19 – bevel gearbox; 20 – driven pulley; 21 – driving pulley; 22 – belt; 23 – main electric motor; 24 – chute; 25 – pneumatic separating channel; 26 – sieve; 27 – cyclone; 28 – centrifugal fan; 29 – fan electric motor; 30 – seed collector; 31 – unshelled fruit collector; 32 – capsule particle collector; 33 – fine particle and dust collector; 34 – electric wires

lining and the outer lining of the crushing cone. This allows the machine to be adapted to process various raw materials while maintaining a stable cleaning quality.

The use of rubber linings in the design minimises seed damage. The eccentric drive mechanism of the crushing cone provides intensive action on the castor fruits, ensuring efficient shelling even at increased productivity levels. The design of the pneumatic separation channel and cyclone ensures the clear separation of seeds, unhulled fruits, capsule fragments, and dust, reducing valuable product losses. Selecting the optimal sieve hole size allows the free passage of seeds while retaining unhulled fruits.

The automated control system reduces the labour intensity, and the convenient arrangement of machine components simplifies the maintenance and

https://doi.org/10.17221/121/2025-RAE

cleaning after operation. Altogether, these technical solutions provide reliability, high productivity, and efficient cleaning of castor seeds.

Numerical simulation for the separation and cleaning process. The numerical simulation of the castor seed separation and cleaning process under the action of the machine's working elements was carried out in Simcenter Star-CCM+ using a deterministic discrete element method (DEM) approach combined with continuum mechanics.

To accurately represent the geometry, contact interactions, and deformation processes in the working zone, the following mesh models were applied: a polyhedral cell generator and a surface mesh generator. The polyhedral cell generator was selected as the primary tool for creating the volumetric computational mesh to ensure high model quality with fewer cells, which is essential for complex geometries involving the contact interaction between castor fruits and machine components. The surface mesh generator was used for preliminary geometry optimisation to achieve uniform surface coverage and better conformity with imported computer-aided design (CAD) models.

The base mesh size of 0.01 m was selected based on the geometric dimensions of castor fruits (length L = 14.8 ± 2.2 mm, width B = 13.5 ± 1.9 mm), providing sufficient spatial resolution while maintaining a moderate computational load.

In Simcenter Star-CCM+, a comprehensive approach was implemented, covering the interaction of solid bodies, the gas environment, and particle contact mechanics. The physical model was based on the Reynolds-averaged Navier-Stokes equations, describing the motion of viscous compressible gas, with the ideal gas state equation. This allowed the accurate modelling of the air behaviour, especially in zones of local compression and acceleration of the airflow in the machine's working chamber. To account for the turbulence, the k-ε model was applied, known for its universality and robustness against computational errors, capable of describing both large and small vortices in the flow.

The motion of castor fruit particles and their fragmentation products was simulated using a Lagrangian multiphase model, where each particle is treated as an independent object with its own kinematic and physical properties. In this context, the castor fruit was modelled as a set of discrete element method (DEM) particles, incorporating models, such as constant density and particle clustering, which allowed the complex internal structure of the fruit to be reproduced, including multicomponent composition and differing strengths of the shell and kernel.

To model the interaction between the particles and the surrounding medium, a multiphase coupling approach was used, including: rolling resistance to simulate the seed rolling behaviour; DEM phase interaction for momentum exchange between the phases; the Hertz–Mindlin contact model to calculate the contact forces; cohesive particles to account for the adhesion and cohesion bonds; the single-particle breakage model to determine the moment of the particle destruction under load.

The calculations were performed in a non-stationary implicit mode, allowing time-dependent load variations to be considered while avoiding instabilities related to large time steps. Gravity was included as a global factor influencing the particle settling, clustering, and the overall efficiency of the subsequent cleaning process.

The castor fruit was represented by constituent particles with a diameter of 3 mm, while the overall fruit diameter was 15 mm. The material properties were specified as follows: Poisson's ratio of 0.35, Young's modulus of 15 MPa, specific cohesive energy per unit volume of 1 200 J/m^3, and tensile and shear strength limits of 2 MPa. For interactions between the seeds, the static friction coefficient was set to 0.52, the normal and tangential restitution coefficients to 0.3, the rolling friction coefficient to 0.001, and no linear cohesion was considered. The interactions between the seeds and steel walls were defined by a static friction coefficient of 0.41, normal and tangential restitution coefficients of 0.5, a rolling friction coefficient of 0.001, and no linear cohesion (Aliiev and Holovchenko 2025). The air phase was characterised by a dynamic viscosity of $1.85 \cdot 10^{-5}$ Pa·s, a turbulent Prandtl number of 0.9, and a molecular weight of 28.96 kg/kmol. The simulation was carried out in three-dimensional space using an unsteady implicit solver. A time step of 0.01 s was applied, and the total duration of the simulation was 1 200 seconds.

The first stage of the simulation involves studying the process of fruit shelling and seed separation under the action of the crushing and reverse cones. The simulation scheme is shown in Figure 3.

The selected factors for this stage include: feeding hole diameter (D_{in}) – 60–140 mm (step – 40 mm); inclination angle of the crushing cone axis (γ) – 0–4°

https://doi.org/10.17221/121/2025-RAE

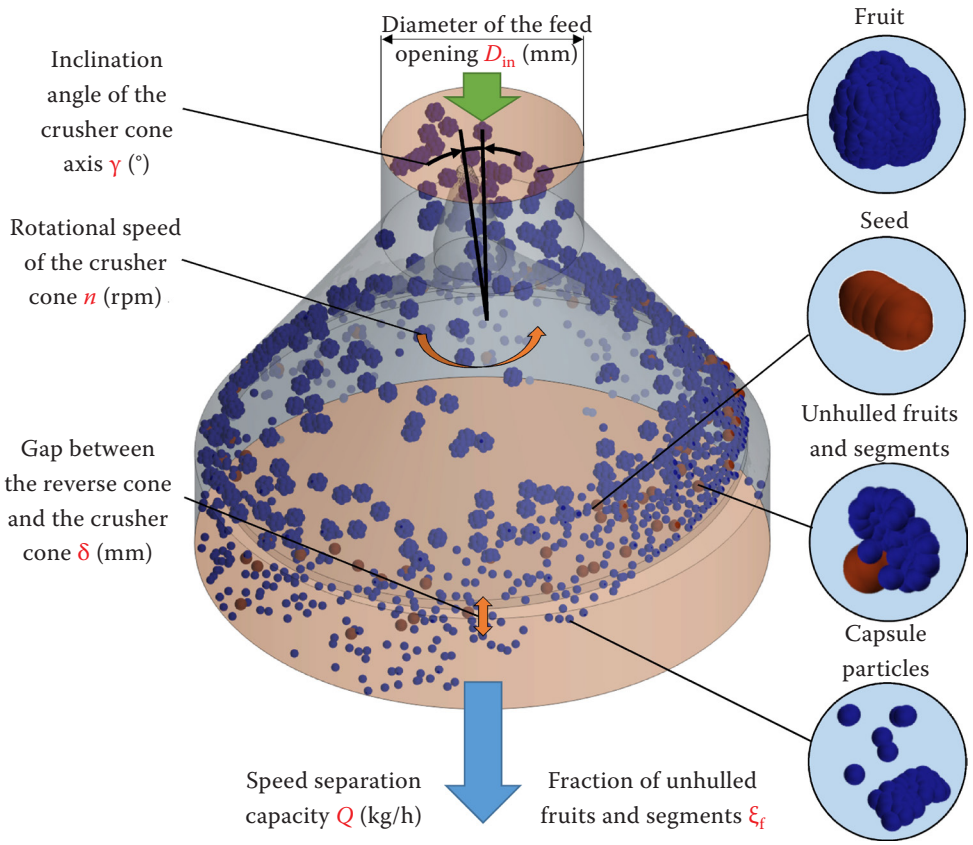

Figure 3. Formulation of the task for the first stage of the numerical modelling of the process of fruit crushing and seed separation under the action of the crushing and reverse cones

(step – 2°); rotational speed of the crushing cone (n) – 200–400 rpm; distance between the reverse and crushing cones (δ) – 0–20 mm (step – 10 mm).

The selected response variables are: the fraction of unshelled fruits and segments (ξ_f); the seed separation productivity (Q).

The second stage of the simulation focuses on the cleaning of the castor seeds from the unshelled fruits, shell residues, and capsule fragments using the aerodynamic cleaning system. This system consists of a pneumatic separation channel with an integrated sieve and a cyclone for removing light impurities from the air stream (Figure 4).

The pneumatic separation channel performs the function of material separation based on the aerodynamic properties. The air stream passing through the channel carries away lighter fractions – shells, capsule fragments, and dust – while heavier castor seeds and some unshelled fruits settle down. To ensure optimal separation conditions, the channel dimensions were set to 220 × 220 mm, corresponding to the recommendations of previous experimental and theoretical studies (Koshulko and Kudriavtsevt 2024; Kudriavtsev 2024). These dimensions provide sufficient cross-sectional area for stabilising the airflow and effectively separating the mixture by size and specific weight.

The cyclone is designed to capture fine particles and dust carried out of the channel. Its design parameters (height, diameter, ratio of inlet to outlet dimensions), Figure 5, were chosen based on prior studies (Wang 2004; Zhao and Su 2018), ensuring a high degree of air cleaning with minimal seed loss.

The sieve in the pneumatic separation channel performs an additional size-based separation function. A bar-type sieve is used to allow efficient seed passage while retaining larger capsule fragments. The gap between the bars is set at 12 mm, which is smaller than the size of the fruits, but larger than the size of the seeds. This minimises the seed loss while effectively removing oversized impurities.

In the framework of the simulation and subsequent experimental studies, the main variable design factor is the sieve inclination angle (β).

https://doi.org/10.17221/121/2025-RAE

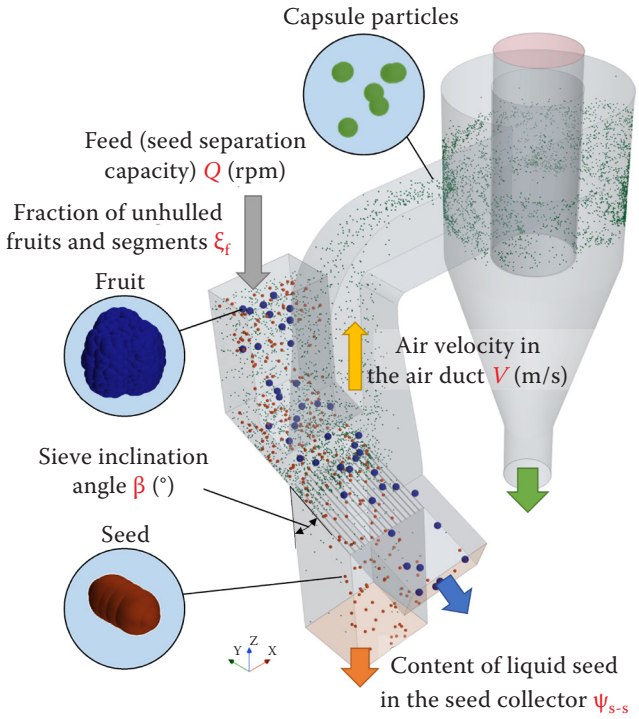

Figure 4. Formulation of the task for the numerical modelling of the seed cleaning process from fruits and particles under the influence of airflow

Adjusting the angle between 10° and 40° (in line with the angle of natural repose, step – 15°) allows control over the separation efficiency and ensures optimal operating conditions of the aerodynamic cleaning system by influencing the particle movement direction and velocity in the airflow.

The input material consists of a mixture of unshelled fruits and segments, seeds, and capsule fragments. Based on the results of the first simulation stage, the mixture composition is: fraction of unshelled fruits and segments: $\xi_f = 0.14$; fraction of seeds: $\xi_s = 0.61$; fraction of capsule particles: $\xi_p = 0.25$.

The seed separation productivity (Q) is one of the investigated factors. According to the first stage of the study, Q ranges from 30 kg/h to 230 kg/h (step – 100 kg/h). The third factor is the air velocity (V) in the pneumatic separation channel, which varies from 2 m/s to 6 m/s (step – 2 m/s).

The response criterion for the second stage is the content of clean seeds in the seed collector (ψ_{s-s}), which was automatically measured in Simcenter Star-CCM+ every 0.1 seconds. The total simulation time was 300 seconds.

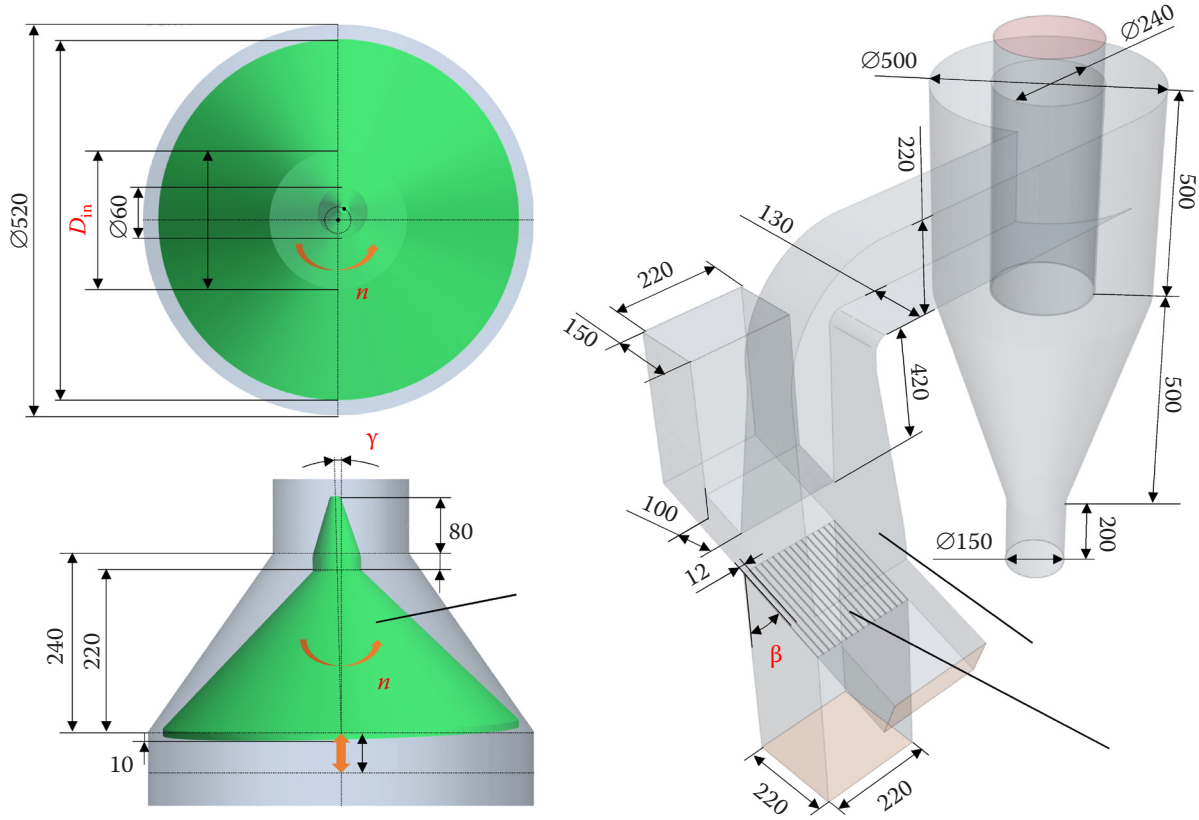

Figure 5. Geometric dimensions of the experimental equipment

https://doi.org/10.17221/121/2025-RAE

The numerical simulation was carried out according to a full factorial design, with each factor varied at three levels.

Experimental castor seed separation process. The test bench for studying the castor seed cleaning machine (Figure 6) is designed for the experimental investigation of the seed separation process from fruits, as well as for cleaning the seeds from impurities and further fractionating the products into appropriate fractions (Figure 7).

The main elements of this unit are the crushing cone and the reverse cone, mounted in a housing with an internal lining (Figure 8).

All the geometric dimensions of the fabricated equipment fully correspond to the dimensions of the model (Figure 5).

Figure 6. Test bench for studying the castor seed cleaning machine
1 – frame; 2 – castor seed separation system from fruits; 3 – loading hopper; 4 – aerodynamic cleaning system; 5 – pneumoseparating channel; 6 – cyclone; 7 – centrifugal fan; 8 – fan electric motor; 9 – main electric motor; 10 – seed collector; 11 – unhulled fruit collector; 12 – capsule particle collector; 13 – fine particle and dust collector; 14 – control unit; 15 – Danfoss Micro Drive frequency converter

Castor fruits (raw material) Capsule particles Seeds

Figure 7. Results of the seed separation from capsules

https://doi.org/10.17221/121/2025-RAE

Figure 8. Individual components of the test bench for studying the castor seed cleaning machine
1 – reverse cone; 2 – crushing cone; 3 – housing with internal lining; 4 – adjustment screw; 5 – sprocket; 6 – chain; 7 – external lining; 8 – distributor; 9 – conical eccentric cup-shaft; 10 – bevel gear; 11 – driven pulley; 12 – driving pulley; 13 – belt; 14 – main electric motor

The operation of the test bench is controlled via a control unit, equipped with Danfoss Micro Drive frequency converters, which allow for the precise adjustment of rotational speed and real-time measurement of the power consumption of the electric motors driving the crushing cone and the centrifugal fan of the aerodynamic cleaning system.

To monitor the airflow speed, a Solomat MPM500 multifunction measuring device was used, while the rotational speed of the crushing cone was measured with a Benetech GM8905 tachometer. The mass of different product fractions obtained during the machine's operation was determined using VP1-Tv electronic scales.

The experiments were conducted under standard ambient conditions: air temperature of 25.0 ± 1.8 °C, atmospheric pressure of 101.3 ± 0.7 kPa, and relative humidity approximately of 50.4 ± 5.1%.

The selected experimental factors were the design and process parameters that have the greatest influence on the separation and cleaning of castor seeds: distance between the reverse and crushing cones (δ) – 0–20 mm (step – 10 mm); rotational speed of the crushing cone (n) – 200–400 rpm (step – 100 rpm); airflow speed (V) – 2–6 m/s (step – 2 m/s).

The chosen response criteria were: machine productivity (Q) in kg/h, determined as the ratio of the mass of the processed material to the operation time; power consumption (P) in watts, recorded directly from the frequency converter data; specific energy consumption (E) in MJ/kg, calculated as the ratio of power (P) to productivity (Q); fraction of unshelled fruits and segments (ξ_f), determined by sampling 300 g of product, repeated three times; content of clean seeds in the seed collector ($\psi_{s\text{-}s}$), also determined by sampling 300 g of product in triplicate. The degree of seed damage is taken into account by the indicator $\psi_{s\text{-}s}$, which represents the content of clean, undamaged seeds collected in the seed collector. This metric allows quantifying losses due to the mechanical damage during the separation and cleaning process. The mass processed in a single experiment was 100 kg.

The experimental studies were conducted according to a Box-Behnken design for three factors, each varied at three levels, resulting in a total of 15 experimental runs. Each run was repeated three times.

Statistical analysis. The methodology for the statistical processing of the numerical simulation and experimental data in Wolfram Cloud involves sequential steps: factor coding, regression model construction, analysis of coefficient significance, model adequacy verification, response surface visualisation, and optimisation. Factors are coded by normalising their natural values to a range from −1 to +1. The regression model, typically second-order, includes linear, quadratic, and interaction terms, and the coefficients are estimated and tested for significance using Student's t-test. Insignificant coefficients are removed, and the model is refined. The model adequacy is verified using an analysis of variance (ANOVA), where the Fisher F-test is applied to determine whether the regression model ad-

https://doi.org/10.17221/121/2025-RAE

equately fits the experimental data; a *P*-value < 0.05 indicates that the model is statistically significant.

The results are visualised using response surfaces (Plot3D), enabling the assessment of the influence of the factors on the output variable. Optimisation is carried out via numerical minimisation/maximisation (FindMinimum/FindMaximum) and the scalar ranking method for multi-criteria tasks. This approach ensures a complete cycle of the experimental data analysis with high accuracy and flexibility.

RESULTS

Determined regression models of the parameters

Numerical simulation. As a result of the numerical simulation, a regression equation was obtained for the seed separation productivity (Q) in kg/h, which has the following form (Figure 10):

$$\begin{aligned} Q^S = &- 240.523 - 0.59051\, D_{in} + 0.002264\, D_{in}^2 + \\ &+ 2.362\, n + 0.00139\, D_{in}\, n - 0.004277\, n^2 + \\ &+ 6.68519\, \gamma - 0.733333\, \gamma^2 + 1.59111\, \delta + \\ &+ 0.0190278\, D_{in}\, \delta + 0.00917222\, n\, \delta - 0.0602\, \delta^2 \end{aligned} \quad (1)$$

where: Q^S – seed separation productivity from numerical simulation (kg/h); D_{in} – diameter of the feed opening (mm); n – rotational speed of the crushing cone (rpm); γ – inclination angle of the crushing cone axis (°); δ – distance between the reverse and crushing cones (mm).

According to Fisher's criterion, $F_{(1)} = 3\,309 > F_t(15, 66, 0.05) = 1.95$, Equation (1) is statistically significant. The coefficient of determination between the obtained equation and the experimental data is $R^2 = 0.991$.

An increase in rotational speed (n) improves the productivity up to a certain limit; however, excessive growth of n leads to saturation and even a decrease in efficiency. This is due to the increase in inertial forces, which can cause the repeated capturing and crushing of the fruits, resulting in higher losses and the overloading of the separation system.

Increasing the feeding diameter (D_{in}) initially enhances the productivity due to the higher material feed rate. However, if the inlet opening is too large, the efficiency of fruit destruction decreases due to the uneven material flow distribution and machine loading beyond the optimal level.

The inclination angle of the crushing cone axis (γ) also has a quadratic effect: up to a certain point, it improves the feeding and fruit destruction, but exceeding the optimal angle reduces the efficiency because the trajectory of particle movement changes, and part of the material may not enter the crushing zone.

The distance between the cones (δ) determines the degree of fruit destruction. Too small a gap leads to over-crushing, higher energy consumption, and a loss of viable seeds, while too large a gap reduces the shelling efficiency and increases the proportion of unshelled fruits in the waste.

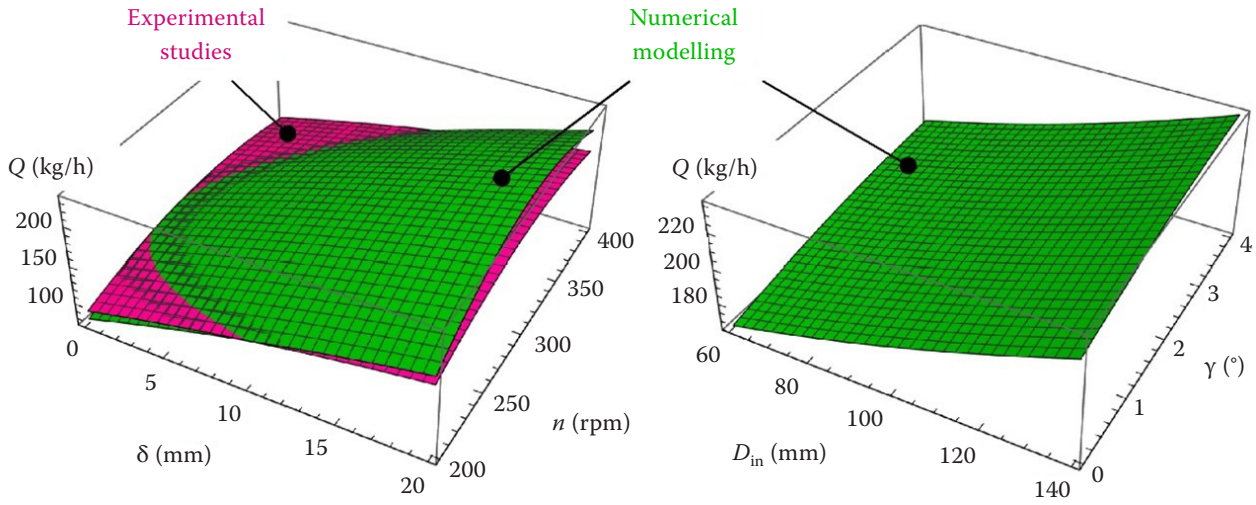

Figure 10. Dependence of the castor seed separation productivity Q on the distance between the reverse and crushing cones δ, the rotational speed of the crushing cone n, the diameter of the feed opening D_{in}, and the inclination angle of the crushing cone axis γ

https://doi.org/10.17221/121/2025-RAE

The regression equation for the fraction of unshelled fruits and segments (ξ_f) has the following form (Figure 11):

$$\xi_f^S = 0.2906 - 0.001992\, D_{in} + 0.00001445\, D_{in}^2 - \\ - 0.0012489\, n + 2.31 \cdot 10^{-6}\, n^2 - 0.0279\, \gamma + \\ + 0.0046852\, \gamma^2 + 0.014887\, \delta + 9.778 \cdot 10^{-6}\, n\, \delta - \\ - 0.000311111\, \gamma\, \delta - 0.000378704\, \delta^2 \quad (2)$$

where: ξ_f^S – fraction of unshelled fruits and segments from numerical simulation; D_{in} – diameter of the feed opening (mm); n – rotational speed of the crushing cone (rpm); γ – inclination angle of the crushing cone axis (°); δ – distance between the reverse and crushing cones (mm).

According to Fisher's criterion, $F_{(2)} = 8\ 904 > F_t(15, 66, 0.05) = 1.95$, Equation (2) is statistically significant. The coefficient of determination between the obtained equation and the experimental data is $R^2 = 0.985$.

The analysis of the equation for the fraction of unshelled fruits showed that reducing this indicator is achieved by increasing the rotational speed and decreasing the gap; however, an optimum is also observed, since excessive speed or too small a gap can cause seed damage and increased energy consumption. The effect of the feeding hole diameter is weak, but also has a quadratic nature – large openings may allow unshelled fruits to pass through without effective processing. The inclination angle of the crushing cone axis has a significant influence – up to a certain value, it reduces the amount of unshelled fruits, but excessive inclination causes the opposite effect.

The regression equation for determining $\psi_{s\text{-}s}$ (the content of clean seed in the seed collector) is presented as follows (Figure 12):

$$\psi_{s\text{-}s}^S = 0.59397 + 0.00319717\, Q - 9.739 \cdot 10^{-6}\, Q^2 + \\ + 0.0035\, V + 0.007938\, \beta - 0.000195\, \beta^2 \quad (3)$$

where: $\psi_{s\text{-}s}^S$ – content of clean seed in the seed collector from numerical simulation; Q – seed separation productivity (kg/h); V – airflow velocity (m/s); β – inclination angle of the sieve (°).

According to Fisher's criterion, $F_{(3)} = 4\ 251 > F_t(10, 17, 0.05) = 2.54$, Equation (3) is statistically significant. The coefficient of determination between the obtained equation and the experimental data is $R^2 = 0.986$.

As the productivity increases, the content of clean seeds also increases up to a certain limit, after which a saturation effect leads to stabilisation or even a decrease in the indicator due to increased losses. The airflow velocity improves the cleaning of seeds from husks; however, excessive airflow can carry away the fine fractions of clean seeds, reducing the product quality. The inclination angle of the pneumatic separator has an optimal range of values at which effective pneumatic separation is ensured; excessive inclination leads to increased seed losses together with light impurities.

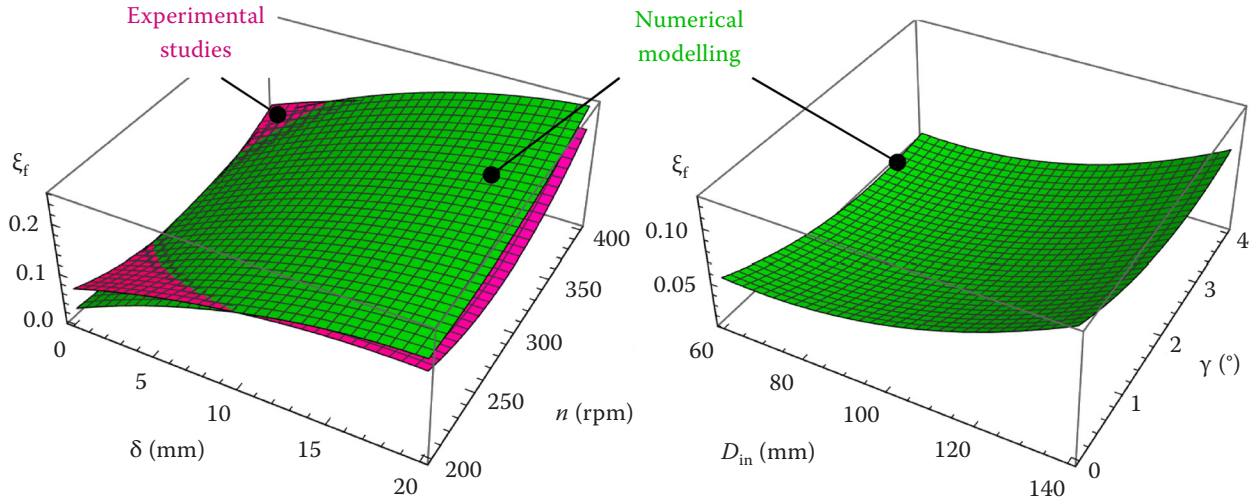

Figure 11. Dependence of the fraction of unhulled fruits (segments) ξ_f on the distance between the reverse and crushing cones δ, the rotational speed of the crushing cone n, the diameter of the feed opening D_{in}, and the inclination angle of the crushing cone axis γ

https://doi.org/10.17221/121/2025-RAE

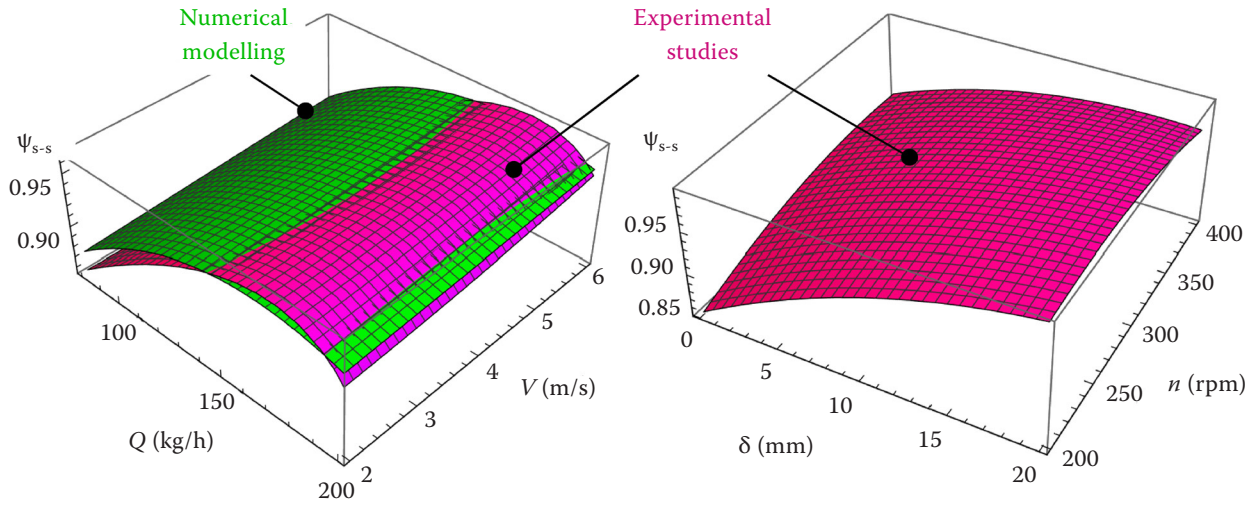

Figure 12. Dependence of the content of clean seeds in the seed collector $\psi_{s\text{-}s}$ on the feed rate (seed separation productivity) Q, air flow velocity V, distance between the reverse and crushing cones δ, and rotational speed of the crushing cone n

Modelling of the experimental data. The regression equation for the productivity of the developed machine, Q (kg/h), is as follows (Figure 10):

$$Q^E = -110.281 + 1.43903\ n - 0.00224805\ n^2 + \\ + 4.93852\ \delta - 0.0568829\ \delta^2 \quad (4)$$

where: Q^E – productivity of the developed machine from experimental data (kg/h); n – rotational speed of the crushing cone (rpm); δ – distance between the reverse and crushing cones (mm).

According to Fisher's criterion, $F_{(4)} = 21\ 755 > F_t(10, 5, 0.05) = 4.74$, Equation (4) is statistically significant. The coefficient of determination between the obtained equation and the experimental data is $R^2 = 0.987$.

The dependence of productivity on the rotational speed and gap has a quadratic nature – as these parameters increase, the productivity rises up to a certain limit, after which it begins to decline due to the worsening conditions for product crushing and transport.

The numerical simulation also considers the influence of the inlet diameter D_{in} and the inclination angle γ, which corresponds to a comprehensive approach to evaluating the processes of grinding and separation (He 2018; Yang et al. 2021). The experiment showed that these factors are less decisive, which is consistent with the findings of Li et al. (2016), where it is noted that the geometry of the working zone has a critical, but fixed influence, while the variable modes n and δ dominate.

The regression equation for the power consumption P (W) of the developed machine in coded form is as follows (Figure 13):

$$P^E = 1\ 315.67 + 0.002832\ n^2 + 92.475\ V + 1.03625\ n - \\ - 0.037125\ \delta\ n - 17.6425\ \delta \quad (5)$$

where: P^E – power consumption of the developed machine from experimental data (W); n – rotational speed of the crushing cone (rpm); V – airflow velocity (m/s); δ – distance between the reverse and crushing cones (mm).

According to Fisher's criterion, $F_{(5)} = 13\ 110 > F_t(10, 5, 0.05) = 4.74$, Equation (5) is statistically significant. The coefficient of determination between the obtained equation and the experimental data is $R^2 = 0.977$.

The power consumption increases with the rise in rotational speed and airflow velocity, which is physically explained by the increase in resistance to movement and the greater effort required for crushing the fruits and moving the material. Increasing the gap reduces energy consumption because it decreases the degree of crushing and the load on the working parts; however, an excessive gap leads to a decline in cleaning quality.

The regression equation for the specific energy consumption E (MJ/kg) of the developed machine is as follows (Figure 14):

https://doi.org/10.17221/121/2025-RAE

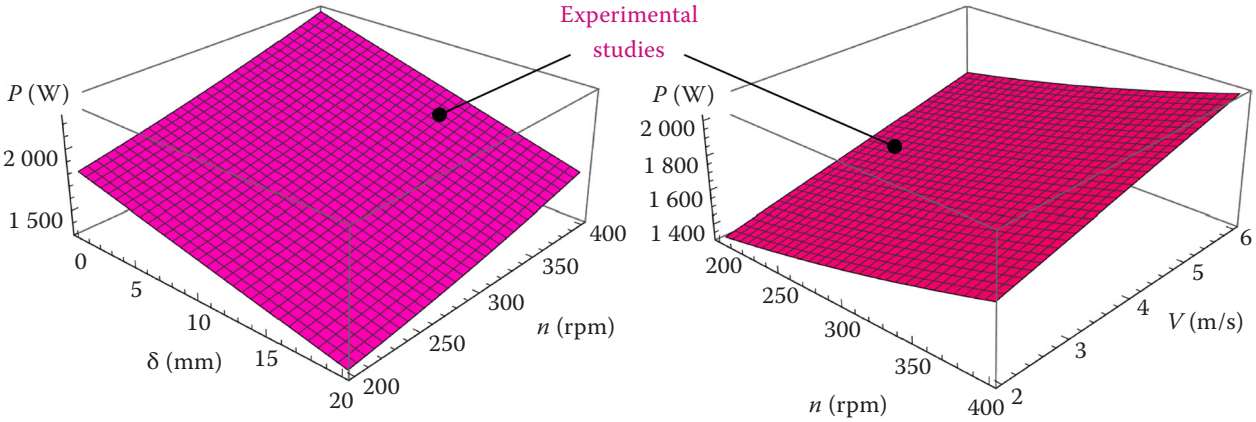

Figure 13. Dependence of the power P consumed by the developed castor seed cleaning machine on the distance between the reverse and crushing cones δ, the rotational speed of the crushing cone n, and the air flow velocity V

$$E^E = 0.1324 + 9.095 \cdot 10^{-7}\, n^2 + 0.001945\, V - 5.017 \cdot 10^{-4}\, n - 1.377 \cdot 10^{-6}\, \delta\, n - 0.003317\, \delta + 7.902 \cdot 10^{-5}\, \delta^2 \quad (6)$$

where: E^E – specific energy consumption of the developed machine from experimental data (MJ/kg); n – rotational speed of the crushing cone (rpm); V – airflow velocity (m/s); δ – distance between the reverse and crushing cones (mm).

According to Fisher's criterion, $F_{(6)} = 625.9 > F_t(10, 5, 0.05) = 4.74$, Equation (6) is statistically significant. The coefficient of determination between the obtained equation and the experimental data is $R^2 = 0.974$.

The specific energy consumption shows an optimum with respect to the rotational speed and gap: at low values of n and δ, the machine operates inefficiently due to underloading, while at excessive values it consumes too much energy crushing and transporting an unnecessarily excessive material flow. Thus, a minimum specific energy consumption is achieved in practical operation with a rational and well-balanced combination of the operating parameters.

These results are consistent with the conclusions of Gbabo et al. (2015) and Yakubu et al. (2020), where it is noted that the energy efficiency of castor dehulling machines is ensured by balancing the intensity of shelling and productivity.

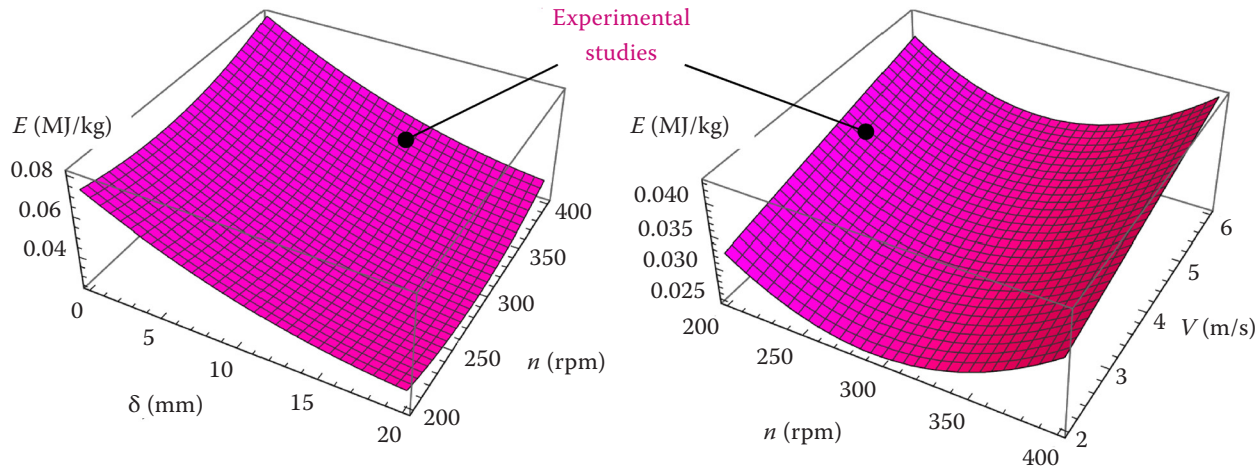

Figure 14. Dependence of the specific energy consumption E by the developed castor seed cleaning machine on the distance between the reverse and crushing cones δ, the rotational speed of the crushing cone n, and the air flow velocity V

https://doi.org/10.17221/121/2025-RAE

The regression equation for the fraction of unshelled fruits (segments) ξ_f has the following form (Figure 11):

$$\xi_f^E = 0.550796 + 6.13042 \cdot 10^{-6} n^2 - 0.0036535 n + 9.25 \cdot 10^{-6} \delta n + 0.00891542 \delta - 0.000285208 \delta^2 \quad (7)$$

where: ξ_f^E – fraction of unshelled fruits and segments from experimental data; n – rotational speed of the crushing cone (rpm); δ – distance between the reverse and crushing cones (mm).

According to Fisher's criterion, $F_{(7)} = 23\,590 > F_t(10, 5, 0.05) = 4.74$, Equation (7) is statistically significant. The coefficient of determination between the obtained equation and the experimental data is $R^2 = 0.984$.

The fraction of unshelled fruits in the experiment confirmed the dependence on the rotational speed and gap, similar to the numerical modelling. An excessive increase in the rotational speed may reduce the cleaning quality due to incomplete capture of particles or disruption of the crushing regime.

The influence of the angles, inlet diameter, and combined effects (γ, $D_{in} \times \delta$, $n \times \delta$) confirms the physical complexity of the process, as described by Anjani (2012) and Alexopoulou et al. (2015), who emphasised that the morphological heterogeneity of castor fruits complicates the predictability of the dehulling process.

The regression equation for the content of clean seed in the seed collector $\psi_{s\text{-}s}$ is as follows (Figure 12):

$$\psi_{s\text{-}s}{}^E = 0.66582 - 1.66417 \cdot 10^{-6} n^2 + 0.000677083 V^2 + 0.0012543 n - 0.00001909 \delta n - 0.00380917 V + 0.000125 \delta V + 0.0143342 \delta - 0.000216417 \delta^2 \quad (8)$$

where: $\psi_{s\text{-}s}{}^E$ – content of clean seed in the seed collector from experimental data; n – rotational speed of the crushing cone (rpm); V – airflow velocity (m/s); δ – distance between the reverse and crushing cones (mm).

According to Fisher's criterion, $F_{(8)} = 138\,068 > F_t(10, 5, 0.05) = 4.74$, Equation (8) is statistically significant. The coefficient of determination between the obtained equation and the experimental data is $R^2 = 0.989$.

The content of clean seed in the seed collector under experimental conditions showed a complex dependence on n, δ, and V, with the presence of quadratic effects and interactions between the parameters. Increasing the airflow velocity up to a certain limit promotes seed cleaning; however, exceeding the critical velocity causes some fine clean seed to be carried away with the light impurities, reducing the yield of the valuable product.

Equations (3) and (8) confirm that: while increasing the productivity or airflow velocity V improves cleaning up to a certain limit, excessive the air velocity leads to losses of small seeds – a phenomenon described by Wang (2004), Zhao and Su (2018), and Kudriavtsev (2024). The inclination of the separation plane β or changes in δ significantly influence the separation of light particles (Tesliuk and Holovchenko 2025).

Summarising the results, it can be noted that the obtained dependencies reflect the physical essence of the crushing and separation process of castor seeds, confirming the non-linear nature of the changes in the main performance indicators of the machine. The interaction of the parameters necessitates the search for optimal operating modes to ensure the maximum productivity with minimal energy consumption and high cleaning quality. The application of numerical modelling combined with experimental research allows for the more accurate assessment of the influence of the design and operational parameters on the process and contributes to the improvement of castor seed cleaning technology.

Optimisation of the design and technological parameters

The comparison of the results from numerical modelling and experimental studies of the process of castor seed separation and cleaning showed satisfactory agreement for the main performance indicators of the machine: productivity Q, fraction of unshelled fruits ξ_f, and content of the clean seed in the seed collector $\psi_{s\text{-}s}$. For the productivity, the correlation coefficient between the numerical and experimental models was 0.89; for the fraction of unshelled fruits – 0.85; and for the content of clean seed – 0.78. Numerical models consider a broader range of factors, allowing a more detailed description of the process, whereas the experimental dependencies are simplified, but confirm the main patterns. The obtained results indicate the adequacy of the developed mathematical models and their suitability for predicting the machine's

https://doi.org/10.17221/121/2025-RAE

performance and optimising the castor seed cleaning process.

For optimising the design and technological parameters of the castor seed cleaning machine, we use the condition of minimising the specific energy consumption and the fraction of unshelled fruits (segments) while maintaining a high content of clean seed in the seed collector:

$$\begin{cases} E(\delta, n, V) \to \min \\ \xi_f(D_{in}, \gamma, \delta, n, V) \to \min \\ \psi_{s\text{-}s}(Q(D_{in}, n, \gamma, \delta), \beta, \delta, n, V) \to \max \end{cases} \quad (9)$$

where: E – specific energy consumption (MJ/kg); δ – distance between the reverse and crushing cones (mm); n – rotational speed of the crushing cone (rpm); V – airflow velocity (m/s); ξ_f – fraction of unshelled fruits and segments; D_{in} – diameter of the feed opening (mm); γ – inclination angle of the crushing cone axis (°); $\psi_{s\text{-}s}$ – content of clean seed in the seed collector; Q – seed separation productivity (kg/h); β – inclination angle of the sieve (°).

Using Wolfram Cloud and the minimisation method of a multiplicative function of a complex of criteria obtained by scalarisation, one of the effective approaches to multi-criteria optimisation was implemented.

This approach allows finding the best combination of factor values to achieve an optimal result simultaneously across several criteria. Its essence lies in reducing a multi-criteria problem to a single-criterion one by constructing a so-called multiplicative objective function that reflects the interrelation among all the criteria.

In cases where it is necessary to optimise several functions simultaneously (for example, minimising the specific energy consumption, the amount of unshelled fruits, and maximising the content of clean seed), instead of optimising each criterion separately, a single aggregated function is used in the form of the product of the relative values of each criterion, normalised to the desired or optimal values, taking into account their weights.

The general form of the multiplicative function is:

$$K = \frac{E(\delta, n, V) - E^{min}}{E^{max} - E^{min}} \frac{\xi_f(D_{in}, \gamma, \delta, n, V) - \xi_f^{min}}{\xi_f^{max} - \xi_f^{min}} \frac{\psi_{s\text{-}s}^{max} - \psi_{s\text{-}s}(Q(D_{in}, n, \gamma, \delta), \beta, \delta, n, V)}{\psi_{s\text{-}s}^{max} - \psi_{s\text{-}s}^{min}} \to \min \quad (10)$$

where: K – multiplicative objective function; E – specific energy consumption (MJ/kg); E^{min} – minimum value of specific energy consumption (MJ/kg); E^{max} – maximum value of specific energy consumption (MJ/kg); ξ_f – fraction of unshelled fruits and segments; ξ_f^{min} – minimum value of fraction of unshelled fruits and segments; ξ_f^{max} – maximum value of fraction of unshelled fruits and segments; $\psi_{s\text{-}s}$ – content of clean seed in the seed collector; $\psi_{s\text{-}s}^{min}$ – minimum value of content of clean seed in the seed collector; $\psi_{s\text{-}s}^{max}$ – maximum value of content of clean seed in the seed collector; D_{in} – diameter of the feed opening (mm); γ – inclination angle of the crushing cone axis (°); δ – distance between the reverse and crushing cones (mm); n – rotational speed of the crushing cone (rpm); V – airflow velocity (m/s); β – inclination angle of the sieve (°); Q – seed separation productivity (kg/h).

Solving Equation (10) together with Equations (1–8) yielded rational values for the design and technological parameters of the castor seed cleaning machine: δ = 10.8 mm; n = 282 rpm; V = 3.6 m/s; D_{in} = 98 mm; γ = 3.6°; β = 20.3° → E = 0.0394 MJ/kg; Q = 163.4 kg/h; P = 1 861 W; ξ_f = 0.099; $\psi_{s\text{-}s}$ = 0.958.

DISCUSSION

The proposed machine design, which integrates mechanical dehulling and subsequent aerodynamic cleaning, addresses several challenges highlighted in the previous literature, particularly the high risk of seed damage and the difficulty of achieving efficient shell removal (Sousa et al. 2017; Shevchenko and Aliiev 2022). The present study demonstrates that the efficiency of the mechanical unit strongly depends on the interaction between the crushing cone and the reverse cone. Regression models reveal that both excessive narrowing and excessive widening of the inter-cone gap (δ) reduce the seed quality – either through over-crushing or insufficient dehulling. These findings corroborate the general principles of seed processing, where optimal compression limits must be maintained to avoid breakage (Yang et al. 2021).

The influence of the rotational speed (n) confirms the trends reported for other impact–friction systems (Cao et al. 2012; Li et al. 2016; Hou

https://doi.org/10.17221/121/2025-RAE

et al. 2018), where the increasing rotor speed improves the shelling up to an optimal value, but subsequently results in a performance decline due to fruit re-crushing, overloading, and instability of particle trajectories. Similar behaviour has been reported for dehulling of Ricinus communis using centrifugal and beater-type systems (Gbabo et al. 2015; Yakubu et al. 2020), which supports the reliability of the DEM-based modelling approach used in this research.

The study also confirms the significance of the feeding opening geometry (D_{in}) and the inclination angle (γ). Their quadratic effects indicate the presence of distinct optima, a characteristic commonly observed in seed-flow systems where particle congestion or irregular trajectory formation can diminish the separation quality (He 2018; Tesliuk and Holovchenko 2025). The developed numerical model reliably predicts these interactions, which is further validated by strong agreement with the experimental data (R^2 values exceeding 0.98 for all the regression equations).

The aerodynamic cleaning stage is shown to be equally critical. Previous studies on the pneumatic separation for various granular agricultural materials emphasise the importance of the air velocity and channel geometry in stabilising the particle flow (Koshulko and Kudriavtsev 2024; Kudriavtsev 2024). The current results confirm that the air velocity (V) has a significant positive effect on removing lightweight capsule fragments, aligning with established aerodynamic sorting principles (Wang 2004; Zhao and Su 2018). However, excessive airflow can entrain small or damaged seeds, underscoring the need for the strict tuning of the airflow intensity – especially given the relatively low density and unique surface characteristics of castor seeds.

The effect of the sieve inclination angle (β) observed in this study supports previously noted tendencies wherein moderate inclination facilitates the controlled seed passage and prevents clogging, while excessive angles promote undesirable acceleration and seed bounce. The optimal interval determined here (approximately 20–30°) fits well within the recommended ranges for bar-type sieves used for oilseed cleaning (Kudriavtsev 2024).

Importantly, the achieved level of seed cleanliness ($\psi_{s\text{-}s} > 0.93$ at optimal settings) demonstrates the effectiveness of combining mechanical and aerodynamic stages. This is essential for downstream processing, as castor oil applications – including biodiesel, lubricants, polyurethane foam production, and pharmaceutical products–require high-quality raw material free from shell residue and contaminants (Ogunniyi 2006; Singh 2011; Carrino et al. 2020). Moreover, minimising the seed damage reduces exposure risks associated with ricin and related toxic compounds (Sousa et al. 2017; Abomughaid et al. 2024), which is crucial for operator safety.

Overall, the integration of numerical modelling, parametric optimisation, and experimental validation presented in this study provides a robust foundation for further technological development. The identified optimal operating modes can serve as the basis for industrial-scale implementation, while the modelling framework can be used to refine future machine modifications or simulate other oilseed crops with similar morphological properties. Future research should focus on long-term operational durability, multi-variety testing under varying moisture contents, and incorporating real-time adaptive control algorithms to further enhance the machine's efficiency and reduce energy consumption.

CONCLUSION

As a result of the numerical modelling and experimental studies of the process of separating and cleaning castor seeds, dependencies were obtained for the productivity of the developed machine Q [Equations (1) and (4)], power consumption P [Equation (5)], specific energy consumption E [Equation (6)], fraction of unshelled fruits (segments) ξ_f [Equations (2) and (7)], content of clean seed in the seed collector $\psi_{s\text{-}s}$ [Equations (3) and (8)] depending on the distance between the reverse and crushing cones δ, rotation frequency of the crushing cone n, diameter of the feed opening D_{in}, inclination angle of the crushing cone axis γ, and airflow velocity V. The performed statistical analysis of the regression equations allowed determining the influence of each studied factor on the target performance indicators of the machine, identifying significant parameters, and constructing adequate analytical models.

The application of the scalarisation method with the minimisation of the multiplicative function in the Wolfram Cloud environment made it possible to establish optimal combinations of factor

https://doi.org/10.17221/121/2025-RAE

values (δ = 10.8 mm; n = 282 rpm; V = 3.6 m/s; D_{in} = 98 mm; γ = 3.6°; β = 20.3°), which ensure the maximum process efficiency, taking into account a set of technological (quality) and energy criteria (E = 0.0394 MJ/kg; Q = 163.4 kg/h; P = 1 861 W; ξ_f = 0.099; $\psi_{s\text{-}s}$ = 0.958). The obtained results confirm the feasibility of further implementation of the proposed castor seed cleaning machine design in industrial practice.

The results of this study also create a foundation for future development. The next stage of research will include scaling the prototype to industrial dimensions, integrating it into a continuous castor seed processing line, and conducting pilot tests under real production conditions. Furthermore, the developed regression models and optimisation methodology can be adapted for improving separation and cleaning machines for other oilseed crops. In this way, the findings contribute to the formation of an integrated technological line for castor seed processing and to the broader utilisation of bio-based raw materials in the agro-industrial sector.

REFERENCES

Abomughaid M.M., Teibo J.O., Akinfe O.A., Adewolu A.M., Teibo T.K.A., Afifi M., Al-Farga A.M.H., Al-Kuraishy H.M., Al-Gareeb A.I., Alexiou A., Papadakis M., Batiha G.E.S. (2024): A phytochemical and pharmacological review of *Ricinus communis* L. Discover Applied Sciences, 6: 315.

Alexopoulou E., Papatheohari Y., Zanetti F., Tsiotas K., Papamichael I., Christou M., Namatov I., Monti A. (2015): Comparative studies on several castor (*Ricinus communis* L.) hybrids: growth, yields, seed oil and biomass characterization. Industrial Crops and Products, 75: 8–13.

Aliiev E., Holovchenko V. (2025): Results of laboratory studies on the physico-mechanical properties of castor fruits and seeds. Tekhnika, Enerhetyka, Transport APK, 1: 7–15.

Anjani K. (2012): Castor genetic resources: A primary gene pool for exploitation. Industrial Crops and Products, 35: 1–14.

Cao Y.H., Li C.Y., Zhang Z.X. (2012): Improvement design and test to key components of castor capsule hulling device. Transactions of the Chinese Society of Agricultural Engineering, 28: 16–22.

Carrino L., Visconti D., Fiorentino N., Fagnano M. (2020): Biofuel production with castor bean: A win–win strategy for marginal land. Agronomy, 10: 1690.

Gbabo A., Lukman A., Kuku A. (2015): Design and performance assessment of a spike toothed drum mechanism for shelling of castor. International Journal of Innovative Science, Engineering & Technology, 2: 6–13.

Gelfand I., Sahajpal R., Zhang X., Izaurralde R.C., Gross K.L., Robertson G.P. (2013): Sustainable bioenergy production from marginal lands in the US Midwest. Nature, 493: 514–517.

He T. (2018): Design and experimental study of squeezing and rubbing castor shelling and cleaning device [Master's Thesis]. Shenyang, China, Shenyang Agricultural University.

Hou J.M., Bai J.B., He T. (2018): Design and experiment of castor dehulling and cleaning device with double curved table. Transactions of the Chinese Society for Agricultural Machinery, 49: 139–147.

Janiszewska D., Olchowski R., Nowicka A., Zborowska M., Marszałkiewicz K., Shams M., Giannakoudakis D.A., Anastopoulos I., Barczak M. (2021): Activated biochars derived from wood biomass liquefaction residues for effective removal of hazardous hexavalent chromium from aquatic environments. GCB Bioenergy, 13: 1247–1259.

Koshulko V., Kudriavtsev I. (2024): Justification of the design of an aerodynamic separator for cleaning sunflower seed mixture waste. Tsentralnoukrainskyi Naukovyi Visnyk. Tekhnichni Nauky, 10: 113–122.

Koutroubas S.D., Papakosta D.K., Doitsinis A. (1999): Adaptation and yielding ability of castor plant (*Ricinus communis* L.) genotypes in a Mediterranean climate. European Journal of Agronomy, 11: 227–237.

Kudriavtsev I. (2024): Numerical simulation of the waste separation process of sunflower seed mixture in the pneumatic separating channel of the aerodynamic separator. Tekhnika, Enerhetyka, Transport APK, 2: 47–55.

Li C.Z., Liu R.K., Cheng X.X. (2016): Structure design and parameters optimization of the roll-rub shelling machine for castor capsule. Journal of Central South University of Forestry and Technology, 36: 110–113.

Ogunniyi D.S. (2006): Castor oil: A vital industrial raw material. Bioresource Technology, 97: 1086–1091.

Román-Figueroa C., Cea M., Paneque M., González M.E. (2020): Oil content and fatty acid composition in castor bean naturalized accessions under Mediterranean conditions in Chile. Agronomy, 10: 1145.

Shevchenko I., Aliiev E. (2022): Precise grading and sorting of sunflower plant materials in industrial facilities. Journal of Central European Agriculture, 23: 327–341.

Singh A.K. (2011): Castor oil-based lubricant reduces smoke emission in two-stroke engines. Industrial Crops and Products, 33: 287–295.

Sousa N.L., Cabral G.B., Vieira P.M., Baldoni A.B., Aragão F.J.L. (2017): Bio-detoxification of ricin in castor bean (*Ricinus communis* L.) seeds. Scientific Reports, 7: 15385.

https://doi.org/10.17221/121/2025-RAE

Tesliuk H., Holovchenko V. (2025): Development of mechatronic systems for targeted separation and selection of seed material. Central Ukrainian Scientific Bulletin: Technical Sciences, 11: 167–178.

Vallejos M., Rondanini D., Wassner D.F. (2011): Water relationships of castor bean (*Ricinus communis* L.) seeds related to final seed dry weight and physiological maturity. European Journal of Agronomy, 35: 93–101.

Vedmedeva K.V., Kavyazina M.Y., Makhova T.V. (2018): Evaluation of castor bean samples by economically valuable traits. Scientific and Technical Bulletin of the Institute of Oilseed Crops NAAS, 26: 39–48 (in Ukrainian).

Von Cossel M., Lewandowski I., Elbersen B., Staritsky I., Van Eupen M., Iqbal Y., Mantel S., Scordia D., Testa G., Cosentino S.L. (2019): Marginal agricultural land low-input systems for biomass production. Energies, 12: 3123.

Wang L. (2004): Theoretical study of cyclone design [Dissertation]. College Station, TX, USA, Texas A&M University.

Wydra S., Hüsing B., Köhler J., Schwarz A., Schirrmeister E., Voglhuber-Slavinsky A. (2021): Transition to the bioeconomy – Analysis and scenarios for selected niches. Journal of Cleaner Production, 294: 126092.

Yakubu A.U., Muhammad U.S., Ishiaka M. (2020): Development and performance evaluation of a castor seed (*Ricinus communis*) shelling machine with a winnowing system. FUOYE Journal of Engineering and Technology, 5: 1–5.

Yang L., Chen H., Xiao J., Fan Y., Song S., Zhang Y., Liu X. (2021): Research on structural–mechanical properties during the castor episperm breaking process. Processes, 9: 1777.

Zanetti F., Monti A., Berti M.T. (2013): Challenges and opportunities for new industrial oilseed crops in EU-27: A review. Industrial Crops and Products, 50: 580–595.

Zhao B., Su Y. (2018): Particle size cut performance of aerodynamic cyclone separators: Generalized modeling and characterization by correlating global cyclone dimensions. Journal of Aerosol Science, 120: 1–11.

Received: July 26, 2025
Accepted: December 16, 2025
Published online: March 16, 2026